All-fiber fused directional coupler for highly efficient spatial mode conversion

Rand Ismaeel,[*] Timothy Lee, Bernard Oduro, Yongmin Jung, and Gilberto Brambilla

Optoelectronics Research Centre, University of Southampton, Southampton, SO17 1BJ, UK

[*]*rmni1g10@orc.soton.ac.uk*

Abstract: We model and demonstrate a simple mode selective all-fiber coupler capable of exciting specific higher order modes in two- and few-mode fibres with high efficiency and purity. The coupler is based on inter-modally phase-matching the propagation constants in each arm of the asymmetric fused coupler, formed by dissimilar fibres. At a specific coupler diameter, the launched fundamental LP_{01} mode is coupled into the higher order mode (LP_{11}, LP_{21}, LP_{02}) in the other arm, over a broadband wavelength range around 1550 nm. Unlike other techniques, the demonstrated coupler is composed of a multimode fiber that is weakly fused with a phase matched conventional single mode telecom fiber (SMF-28). The beating between the supermodes at the coupler waist produces a periodic power transfer between the two arms, and therefore, by monitoring the beating while tapering, it is possible to obtain optimum selection for the desired mode. High coupling efficiencies in excess of 90% for all the higher order modes were recorded over 100 nm spectral range, while insertion losses remain as low as 0.5 dB. Coupling efficiency can be further enhanced by performing slow tapering at high temperature, in order to precisely control the coupler cross-section geometry.

OCIS codes: (060.0060) Fiber optics and optical communications; (060.1810) Buffers, couplers, routers, switches, and multiplexers.

References and links

1. D. J. Richardson, J. M. Fini, and L. E. Nelson, "Space-division multiplexing in optical fibres," Nat. Photonics **7**, 354–362 (2013).
2. R. Ryf, S. Randel, A. H. Gnauck, C. Bolle, A. Sierra, S. Mumtaz, M. Esmaeelpour, E. C. Burrows, R. Essiambre, P. J. Winzer, D. W. Peckham, A. H. McCurdy, and R. Lingle, "Mode-division multiplexing over 96 km of few-mode fiber using coherent 6 × 6 MIMO processing," J. Lightwave Technol. **30**, 521–531 (2012).
3. S. Leon-Saval, T. Birks, J. Bland-Hawthorn, and M. Englund, "Multimode fiber devices with single-mode performance," Opt. Lett. **30**, 2545–2547 (2005).
4. S. Leon-Saval, A. Argyros, and J. Bland-Hawthorn, "Photonic lanterns: a study of light propagation in multimode to single-mode converters," Opt. Express **18**, 8430–8439 (2010).
5. S. Leon-Saval, N. Fontaine, J. Salazar-Gil, B. Ercan, R. Ryf, and J. Bland-Hawthorn, "Mode-selective photonic lanterns for space-division multiplexing," Opt. Express **22**, 1036–1044 (2014).
6. N. K. Fontaine, S. G. Leon-Saval, R. Ryf, J. R. S. Gil, B. Ercan, and J. Bland-Hawthorn, "Mode-selective dissimilar fiber photonic-lantern spatial multiplexers for few-mode fiber," Optical Communication (ECOC 2013), 39th European Conference and Exhibition, pp. 1, 3, 22–26 Sept. 2013
7. A. M. Vengsarkar, J. A. Greene, and K. A. Murphy, "Photoinduced refractive-index changes in two-mode elliptical-core fibers: sensing applications," Opt. Lett. **16**, 1541–1543 (1991).

8. C. D. Poole, C. D. Townsend, and K. T. Nelson, "Helical-grating two-mode fiber spatial-mode coupler," J. Lightwave Technol. **9**, 598–604 (1991).
9. H. G. Park and B. Y. Kim, "Intermodal coupler using permanently photoinduced grating in two-modeoptical fiber," Electron. Lett. **25**, 797–799 (1989).
10. F. A. Castro, S. R. M. Carneiro, O. Lisboa, and S. L. A. Carrara, "Two-mode optical fiber accelerometer," Opt. Lett. **17**, 1474–1475 (1992).
11. S. Y. Haung, J. N. Blake, and B. Y. Kim, "Perturbation effects on mode propagation in highly elliptical core two-mode fibers," J. Lightwave Technol. **8**, 23–33 (1990).
12. J. N. Blake, S. U. Huang, B. Y. Kim, and H. J. Shaw, "Strain effects on highly elliptical core two-mode fibers," Opt. Lett. **12**, 732–734 (1987).
13. W. V. Sorin, B. Y. Kim, and H. J. Shaw, "Highly selective evanescent modal filter for two-mode optical fibers," Opt. Lett. **11**, 581–583 (1986).
14. R. C. Youngquist, J. L. Brooks, and H. J. Shaw, "Two-mode fiber modal coupler," Opt. Lett. **9**, 177–179 (1984).
15. M. Vaziri and C. Chen, "An etched two-mode fiber modal coupling element," J. Lightwave Technol. **15**, 474–481 (1997).
16. Y. Shou, J. Bures, S. Lacroix, and X. Daxhelet, "Mode separation in fused fiber coupler made of two-mode fibers," Opt. Fiber Technol. **5**, 92–104 (1999).
17. K. Y. Song, I. K. Hwang, S. H. Yun, and B. Y. Kim, "High performance fused-type mode selective coupler for two-mode fiber devices," in *Opt. Fibre Commun. Conf.*, Baltimore, 7-10 Mar (2000).
18. K. Y. Song, I. K. Hwang, S. H. Yun, and B. Y. Kim, "High performance fused-type mode-selective coupler using elliptical core two-mode fiber at 1550nm," IEEE Photon. Technol. Lett. **14**, 501–503 (2002).
19. Y. Jung, R. Chen, R. Ismaeel, G. Brambilla, S. Alam, I. Giles, and D. Richardson, "Dual mode fused optical fiber couplers suitable for mode division multiplexed transmission," Opt. Express **21**, 24326–24331 (2013).
20. S. Yerolatsitis, I. Gris-Sánchez, and T. Birks, "Adiabatically-tapered fiber mode multiplexers," Opt. Express **22**, 608–617 (2014).
21. K. Chiang, "Effects of cores in fused tapered single-mode fiber couplers," Opt. Lett. **12**, 431–433 (1987).
22. G. Brambilla, "Optical fiber nanowires and microwires: a review," J. Opt. **12**, 043001 (2010).
23. A. W. Snyder and X. H. Zheng, "Fused couplers of arbitrary cross-section," Electron. Lett. **21**, 1079–1080 (1985).
24. S. Lacroix, F. Gonthier, and J. Bures, "Modeling of symmetric 2× 2 fused-fiber couplers," Appl. Opt. **33**, 8361–8369 (1994).
25. F. P. Payne, C. D. Hussey, and M. S. Yataki, "Polarisation analysis of strongly fused and weakly fused tapered couplers," Electron. Lett. **21**, 561–563 (1985).
26. H. Chang, T. Lin, and T. Wu, "Accurate coupling coefficients for fiber couplers with weakly fused cross sections," Appl. Opt. **34**, 6168–6171 (1995).

1. Introduction

Single mode fibers (SMF) propagating only a fundamental mode have been used as a long-haul transmission medium in optical fiber communications and developed for many photonics applications, including sensors, fiber lasers, spectroscopy and bio-medical uses. Recently, the mode division multiplexing (MDM) technique [1,2] has been introduced and developed rapidly to break through the predicted capacity crunch, and the interest in high-order modes and their potential use in MDM systems has increased significantly. Here, one of the most important issues in MDM system is the mode multiplexer and demultiplexer, since the current MDM systems involves many free space bulk optical components which are not only expensive and highly lossy, but also make it difficult to increase the number of spatial modes. An elegant solution to this problem has been represented by photonic lanterns [3–6], which allow for the simultaneous combination of N singlemode fibre outputs in a single multimode fibre supporting N modes. A more challenging task has been represented by the add-drop multiplexers for single channels. For this task, Therefore, all-fiber fused modal couplers promisies a cheap, compact and efficient mode conversion approach.

Over twenty years ago, such mode selective couplers (MSCs) had been introduced as an essential building block for a number of multimode fiber devices such as sensors, accelerometers, strain gauges, amplitude modulators, frequency shifters, and chromatic dispersion compensators [7–12]. The principle of the coupler is to phase match the fundamental mode in one fiber with a high-order mode in a few-mode fiber (FMF) and so achieve conversion to the higher-

#207299 - $15.00 USD Received 27 Feb 2014; revised 7 Apr 2014; accepted 23 Apr 2014; published 6 May 2014

order mode. Several techniques were suggested and implemented to achieve this mode conversion, including polished couplers [13], stress induced modal couplers [14] and fused etched multi-mode couplers [15, 16]. One interesting approach [17, 18] was to use a tapered two mode fiber (TMF) to serve as a single mode fiber which was then fused together with another TMF which had been pre-etched to remove the degeneracy between the high order modes [19]. However, the fiber modal coupler was realized for just two mode groups and the etching process resulted in a fragile fiber. Recently, a new approach suggested a device made by tapering few fibres which were then fused in a fluorine-doped silica capillary. In such configuration the fused fibres take the role of a core of a multimode fibre, in which three individual modes could be separately excited [20]. In this paper, therefore, we further explore the possibility of obtaining an efficient mode conversion into high order modes with high modal purity, by using asymmetric fiber couplers formed by fusing pre-tapered SMF and either two or four mode fiber (FMF).

2. Working principle

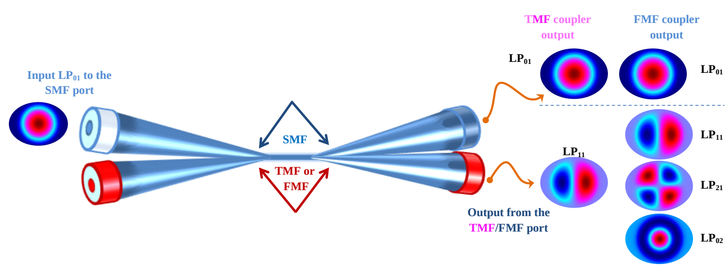

Fig. 1. Schematic of the MSC: light is launched in the SMF port; the LP_{11} is expected to be preferentially excited at the TMF output port, while the uncoupled fundamental LP_{01} will propagate along the SMF. For the FMF, it is possible to select any of the modes that propagates in the FMF by choosing the SMF pre-tapering diameter.

Here, we present a simple, mode selective coupler manufactured via a straightforward two step process. The input light is launched into a telecom fiber (SMF-28) that has been pre-tapered and fused to a step index TMF (core/cladding diameter = 19.7/125μm, NA = 0.12) or FMF (core/cladding diameter =26.1/125μm, NA = 0.12) as shown in Fig. 1. Clearly, the use of a conventional telecom SMF instead of the TMF to support the input LP_{01} mode is especially convenient for telecommunication systems since it would be compatible for the wide range of devices optimized to interface with telecom fibers. In this paper we use the weakly-fused coupler approximation to model and demonstrate the mode conversion. The coupling region for the weakly fused 2×2 coupler is treated as two touching circular cylinders. We chose the weak fusion technique to maintain the geometry of both fibres and therefore achieve accurate index matching. By using this technique, we can directly (and selectively) couple the input LP_{01} mode from the telecom fiber to the other higher order mode supported in the TMF (or FMF).

Tapering the SMF fiber is essential for the mode conversion to occur, since two different fibers (and hence different propagation constants) are used in manufacturing the coupler, Therefore tapering the SMF into a specific diameter will match the propagation constants for the LP_{01} mode in the SMF with the desired higher order mode in the TMF/FMF. The power distribution at any position z along the coupling region of the coupler, is given by two functions $P_1(z)$ and $P_2(z)$, which give the power in the SMF and TMF/FMF arm respectively. For our case of asymmetric fibres, where the propagation constant β_1 of the fundamental mode in the

#207299 - $15.00 USD Received 27 Feb 2014; revised 7 Apr 2014; accepted 23 Apr 2014; published 6 May 2014

SMF is phase matched with the β_2 of the high-order mode in the multimode fibre, the phase mismatch $\Delta\beta = \beta_1 - \beta_2$ is zero and so the power distribution reduces to $P_1(z) \propto \cos^2(\kappa z)$, $P_2(z) \propto \sin^2(\kappa z)$ indicating a complete periodic power transfer between the two fibers in the lossless case. κ is the coupling coefficient which depends on the index profile of the fibres and the cross-section geometry (i.e the distance between the cores of the two fibres). The power in each arm would therefore depend on these three factors; the geometry, index and the coupling region length. Although in this work we match the diameters of the fibres composing the coupler close to the ideal value, any change in the size or the surrounding of the fibers would introduce a nonzero phase mismatch $\Delta\beta \neq 0$ which limits the fraction of the input power coupled into the higher-order mode. Therefore, we attempted to optimize these three parameters to maximise the possible coupling efficiency. In our modelling, we adapted a three layer system comprised of the coupler cores, cladding and air regions. As the core-cladding interface could still affect the behaviour of the supported modes by providing guidance between the cladding and the external air [21], the overall structure of the couplers should be considered as strongly guiding.

3. Modelling

Firstly, the mode effective indices were calculated at different fiber diameters for step index profiles in order to find the optimum diameter at which the LP_{01} modes are phase matched to the desired higher order mode.

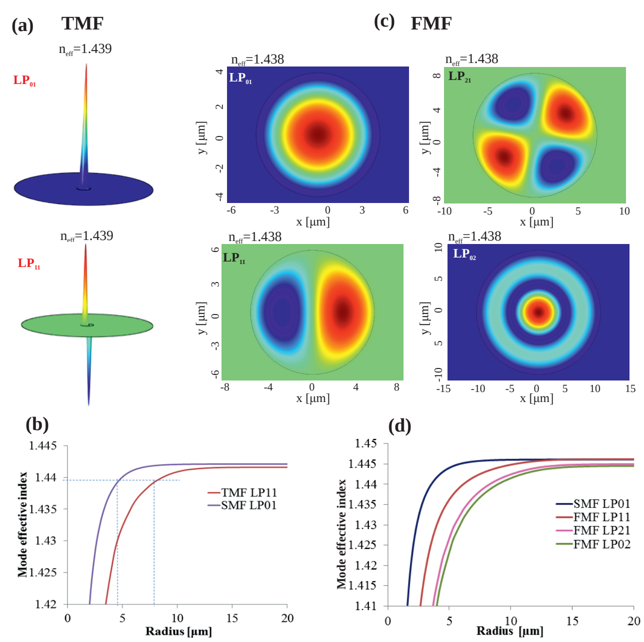

Fig. 2. (a) The electric field component (x direction) of the phase matched modes LP_{01} in the SMF port and the LP_{11} in the TMF port.(b) the phase matching graphs for the LP_{01} in the SMF and the LP_{11} in the TMF. (c) The electric field component of the LP_{01} in the SMF and the LP_{11},LP_{21},LP_{02} in the FMF port. (d) The effective index matching graph for the LP_{01} in the SMF and the desired mode in the FMF (all the modelling was performed using geometrical parameters obtained experimentally,The dotted line represents the dimensions chosen for the fabricated coupler.)

The phase matching curves in Figs. 2(b) and 2(d) indicate that the SMF should be pre-tapered to a diameter of 79 μm to phase match to the LP_{11} mode in the TMF and pre-tapered to 78 μm ,45 μm and 33 μm to phase match the LP_{11}, LP_{21} and the LP_{02} in the FMF respectively.After fabrication, the index profiles of both fibers (which was measured using a S-14 profilometer) was imported into the simulation software COMSOL to solve for the modes numerically and thus confirm the phase matching condition between both modes Figs. 2(a) and 2(c).

The results from both methods confirm that the ratio between the SMF to the TMF diameters should be around 0.63 as shown in Fig. 2(a). Since the scalar LP_{11} mode is actually composed of multiple vectorial modes (TE_{01}, TM_{01} and and the two hybrid HE_{21} modes), the difficulty in selecting one specific vectorial mode could be a source of loss. To minimise this issue, a long tapering length was used to separate the modes that have different group velocity. The optimum coupler length was optimized experimentally, until the maximum power transfer was obtained. The same technique was exploited to efficiently couple the modes in the FMF.

In order to determine the possibility of obtaining high conversion efficiency, the TMF coupler cross-section was measured by scanning electron microscopy as shown in Fig. 3(a), which confirms that the coupler cross-section is weakly fused as required for the expected efficient power transfer between the two coupler arms. Figure 3(b), the result of the modelling, shows that it is possible to transfer most of the power from the phase matched SMF to the TMF in the form of the LP_{11} mode. The analytical results shows that a maximum transfer would accrue around a coupler diameter of 10 μm and coupler length of 25 μm, which are the parameters of giving the first peak of the beating oscillations.

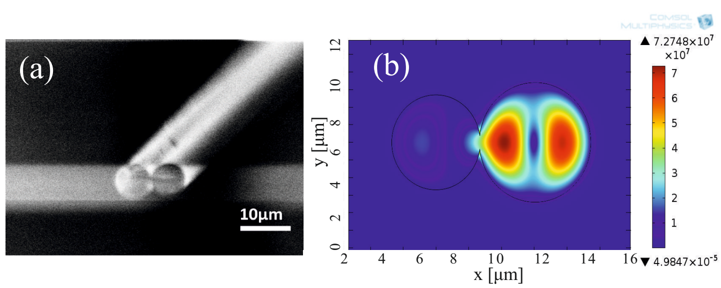

Fig. 3. (a) Scanning electron microscope image of the weakly fused coupler cross section. (b) Simulated resulted for specific coupler diameter, most of the power is expected to be transferred to the output of the coupler as LP_{11}.

To determine the dependency of the coupling efficiency between the LP_{01} and the LP_{11} on the change in the tapering diameter, we solved the following system of coupled equations:

$$\frac{d}{dz}\begin{pmatrix} A_1(z) \\ A_2(z) \end{pmatrix} = \begin{pmatrix} i\frac{\Delta\beta}{2} & i\kappa \\ i\kappa & -i\frac{\Delta\beta}{2} \end{pmatrix}\begin{pmatrix} A_1(z) \\ A_2(z) \end{pmatrix} \tag{1}$$

where z represents the distance along the coupler length, A_1, A_2 are the slowly-varying field amplitudes in the two fibres forming the coupler, κ is the coupling coefficient, which is approximated as half the difference between the propagation constants of the symmetrical (even) and antisymmetrical (odd) modes on the composite waveguide. The value of κ was calculated to be 5130 m^{-1} assuming that the coupler cross-section is composed of two touching circular cylinders (weakly fused asymmetric coupler) [26].

Figure 4(a) shows that the efficiency drops significantly at diameters smaller than the phase matching diameter, while at larger diameters this dependency is less significant, this behaviour is related to the rapid drop in the mode effective index versus the tapering diameter as a result

#207299 - $15.00 USD Received 27 Feb 2014; revised 7 Apr 2014; accepted 23 Apr 2014; published 6 May 2014

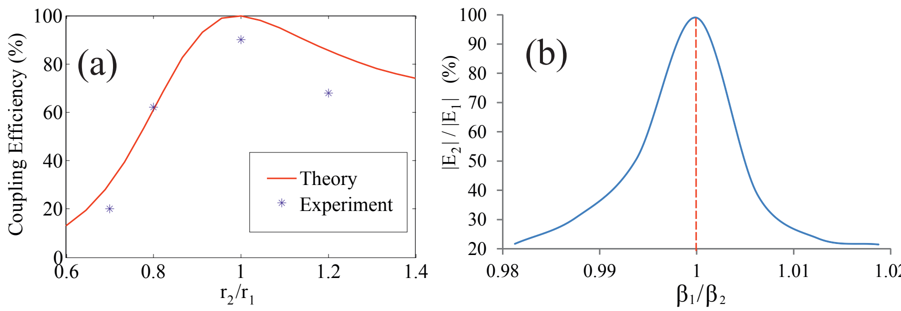

Fig. 4. (a) Coupling efficiency versus the deviation from the ideal SMF phase matching diameter at the coupler waist, r1 is the ideal SMF diameter and r2 represents smaller or larger diameter than the ideal diameter(b) The electric field amplitude ratio at the fibre centres, $|E_2|/|E_1|$, versus the ratio between both fibres propagation constants β_1/β_2.

of the effect of the surrounding air as the new cladding medium at small diameter. The coupling efficiency is also dependent on the degree of fusion and will be discussed in future work. Although increasing the degree of fusion would increase the coupling between the two modes, it will change the weakly fused coupler cross-section and therefore it will be more difficult to find the phase matching diameters of the fibres composing the coupler.

In the case of strong fusion, the effects of the unequal propagation constants on the field distribution is illustrated in Fig. 4(b) which gives the electric field amplitude ratio, E_2/E_1, versus the ratio between the two unequal propagation constants, where E_1 and E_2 are the electric field amplitudes at the centres of each fiber composing the coupler, respectively. It is seen that $|E_2|/|E_1|$ depends strongly on β_1/β_2 and achieving high coupling efficiency above 90% requires the difference between β_1 and β_2 to be within a strict tolerance of $< 0.5\%$.

4. SMF-TMF coupler experiment

We first discuss the experiments for the SMF-TMF coupler here, followed by the SMF-FMF coupler in the next section. The SMF diameter was pre-tapered to 78 μm over a length of 2 cm with losses smaller than 0.1 dB. The pre-tapered fiber was then carefully aligned (without twisting) with the TMF and fused together using the modified flame brushing technique [22]. During fabrication, both the tapering temperature and speed were varied, with the temperature set to 1555 °C at the beginning of the process and reduced down to 1320 °C for diameters smaller than 15 μm. The speed of the tapering was reduced 3 times after halfway through the tapering to maintain the shape of the coupler cross-section during pulling. Meanwhile, the power transfer between both fibres was monitored in-real-time using a power meter attached to both output ports, while light from a 1550 nm laser diode source was launched into the SMF input port. The recorded data in Fig. 5(a) shows the power transfer between the LP_{01} in the SMF and the LP_{11} in the TMF.

In this experiment, tapering was stopped at the point of maximum power exchange, i.e. when the output of the TMF was maximized. When tapering continued we noticed a sinusoidal power transfer between the two output ports Fig. 5(a), which occurs as a result of the beating between the two phase matched modes, while tapering continues even further,the frequency of the beating would decrease, which would decrease the wavelength range at the region for which the LP_{11} operates, therefore, it is essential to stop tapering at the point at which the first power transfer maxima is observed, in order to obtain the broadband operation range for the selected mode. From the figure above, The insertion loss in the TMF, calculated (from the power me-

#207299 - $15.00 USD Received 27 Feb 2014; revised 7 Apr 2014; accepted 23 Apr 2014; published 6 May 2014

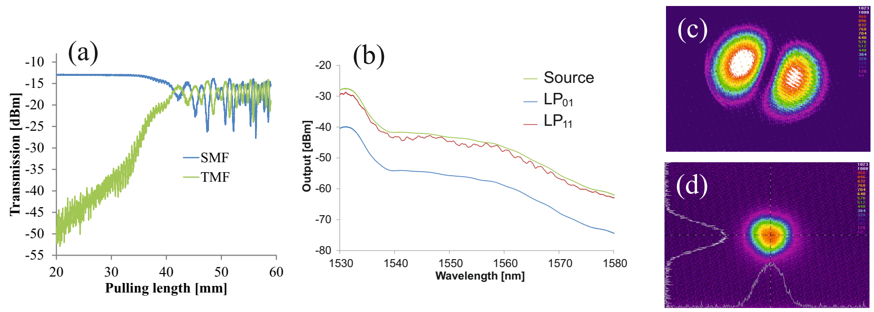

Fig. 5. (a) Power transfer between the two arms of the coupler against pulling length: a periodic power transfer between the output ports is observed. (b) Output spectra of the two arms of the coupler. Far field images of the MSC output at λ ≈1550 nm from the (c) TMF port and (d) SMF port.

ter reading), as the difference between the TMF output at time t (where t represents the time when pulling was stopped) and the SMF output at t = 0 (when pulling started), is estimated to be smaller than 0.4 dB and can be attributed to coupling to other high order modes, or index mismatch.

The transmission of the coupler was measured over a wavelength range around 1550 nm, using a spectrum analyser (Yokogawa, AQ6370) and an amplified spontaneous emission (ASE) source connected to the SMF input port. Figure 5(b) shows that the output power from the TMF arm of the coupler is 12 dB (16 times) higher than that of the SMF over the 50 nm wavelength range shown, which verifies broadband operation and a strong power transfer between the two arms of the coupler. In order to confirm that the output of the TMF arm is actually in the LP_{11} mode, the TMF arm of the coupler was aligned to a CCD camera using an XYZ linear translation stage. A $\times 30$ objective lens was placed between the output port of the coupler and the camera to focus light into the camera. The whole setup was shielded by a foil cover acting as a Faraday cage against external noise sources. Figure 5(c) shows that the LP_{11} mode is observed at the TMF output port as expected, while the LP_{01} dominates the SMF output Fig. 5(d). The far field images prove a good LP_{11} mode purity. A simple intensity level comparison between the maximum and the centre of the mode, as well as from the tight bend technique as described in [18], confirm that the fraction of power at the TMF output in the fundamental mode is smaller than 6%. The mode purity was confirmed by the bending loss scheme with a modal extinction ratio of $< 11dB$ Moreover,The pattern of the LP_{11} output shows an interference pattern, the reason for this interference could be the existence of the LP_{01} in the output of TMF, due to mismatch in the coupler parameters resulted from some variation in the taper geometry, especially in the transition region of the coupler. Further more the LP_{11} pattern shows a small degree of asymmetry that could be another sign of the existence of the LP_{01} in the output of the TMF.

5. SMF-FMF coupler experiment

The same experimental procedure was repeated to excite the higher order modes in a FMF. Initially, the SMF was fused with the TMF over a 30 cm length without any pre-tapering, but it was noticed that the LP_{01} mode dominated the output from the FMF port of the resulting coupler, with a modal purity $> 90\%$ and a coupling efficiency (The coupling efficiency was estimated based on the amount of power coupled from the SMF to the TMF (FMF), and it was calculated based on the power of each port) in the region of 96%.

To generate the higher order modes (LP_{11},LP_{21},LP_{02}), we pre-tapered the SMF to diameters

#207299 - $15.00 USD Received 27 Feb 2014; revised 7 Apr 2014; accepted 23 Apr 2014; published 6 May 2014

of 79 μm,45 μm and 33 μm respectively. The pre-tapered SMF fiber was then fused to the FMF until maximum power transfer between the two output ports was observed, with the length of the fused region selected to be 15 mm for the LP_{11} and 35 mm for the rest of the modes. Longer fusion lengths were required for the LP_{21} and LP_{02} modes to overcome the coupling losses resulting from the bigger geometrical difference between the cores of both fibers at the coupler waist region.The results obtained from the SMF-FMF coupler are shown in Fig. 6. Different pulling lengths were required for each coupler, and tapering was occasionally only stopped after several full power transfer cycles in order to ensure that the two fibres were indeed fused together. Figures 6(a), 6(c), and 6(e) show that the total insertion losses for all the three couplers were less than 0.5dB.

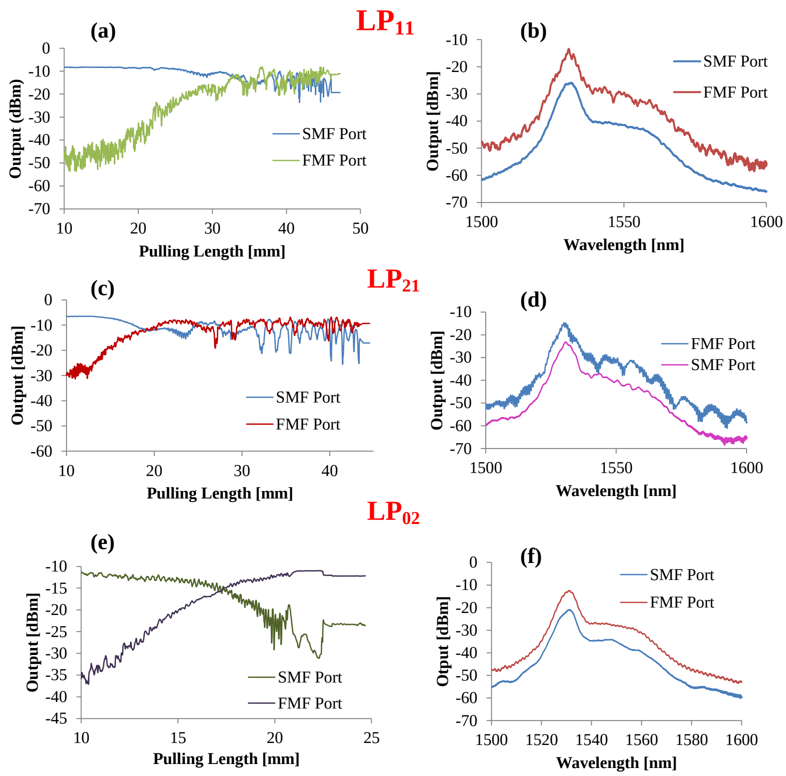

Fig. 6. Power transfer between the two arms of the coupler against pulling length for the (a) LP_{11}, (c) LP_{21}, (e) LP_{02} modes. Output spectra of the two arms of the coupler for the (b)LP_{11}, (d) LP_{21}, (f) LP_{02} modes.

All the three higher order modes supported by the FMF were excited with high coupling efficiencies of 91%,95% and 92% for the LP_{11},LP_{21} and LP_{02} respectively as shown in Figs. 6(b), 6(d), and 6(f). The purity of the modes was verified by the tight bend approach, as well as the far field image field intensity, to be in excess of 92% in all cases, and the performance of the coupler was tested over different wavelengths, at which they all showed coupling efficiencies above 90% as depicted in Fig. 7.

Although we assume that both propagation constants for the matched modes are similar, some difference can be introduced experimentally due to coupler cross-section changes. Since the proposed method here involves changing the geometry of the different fibers in order to achieve phase matching, it is important to maintain the original shape of the fibers the weak fusion. This can be controlled by using a high fusion temperature and relatively fast tapering at the beginning of the process while reducing both of the temperature and the speed at the end of the process. Changing the cross-section could lead to a significant decrease in the coupled power

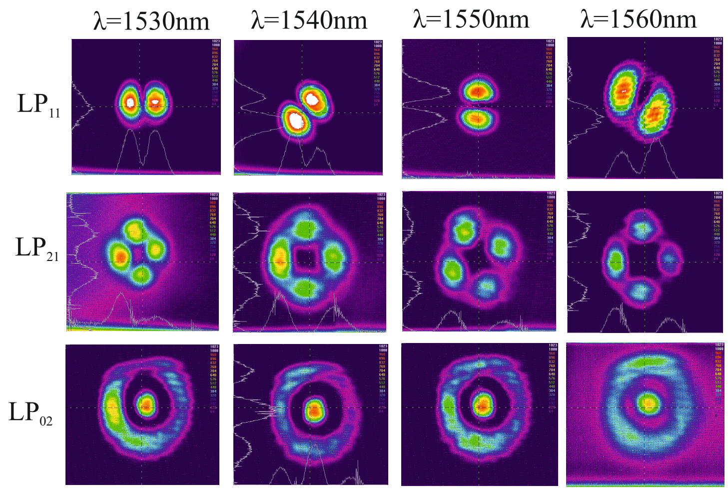

Fig. 7. CCD images of the LP_{11}, LP_{21} and LP_{02} modes excited in the FMF at different launching wavelengths.

to the selected higher order mode, as the modelling has indicated. This technique would also maintain the polarization dependency of the coupler, where a small difference in the output port power less than $1dB$ for all the modes selected was noticed between using the two orthogonal polarizations of the injected light. Moreover, the asymmetric coupler can be applied to convert between specific orthogonal degenerate modes, the X and Y polarizations of the modes (LP_{11} and the LP_{21}) propagating in the coupling region would actually have slightly different propagation constants $\Delta\beta$, due to the slight circular asymmetry in their field distribution and hence overlap integrals between the cores (which determine coupling). This effect would be more noticeable with a stronger index contrast, and also if the cores are nearer together. However, since these value of $\Delta\beta$ is relatively small between the two degenerate modes, its challenging to excite one mode without the other experimentally, since this will require a precise geometry, which is difficult to obtain with the currently available facilitys which is difficult to obtain with the currently available facilities. However, in a real system aspect, an elliptical core few-mode fiber couplers could be one of the solutions to solve the mode degeneracy. Secondly, 90° concatenation of two LP_{11} mode coupler can be examined by actively splicing two modal couplers and ensuring 90° mode orthogonally.

6. Conclusion

In summary, we have modelled and experimentally demonstrated a high coupling efficiency between the fundamental mode and the selected higher order mode in a mode selective coupler composed of a SMF-28 telecom fiber and a TMF or FMF, at telecom wavelengths around 1.55 μm. The phase matching diameter was calculated for a three layer system so that both of the fundamental mode and the selected higher order mode would have equal propagation

#207299 - $15.00 USD Received 27 Feb 2014; revised 7 Apr 2014; accepted 23 Apr 2014; published 6 May 2014

constant, therefore helping to maximise the power transfer which could be obtained. Meanwhile, low insertion losses and high coupling efficiency were ensured by using a variable speed/temperature tapering process to maintain the shape of the waist of the coupler.

Acknowledgments

G. Brambilla gratefully acknowledges the Royal Society (London) for his University Research fellowship. The authors acknowledge partial support of this research by the European Communities 7th Framework Programme under grant agreement 258033 (MODE-GAP) for the fabrication of few mode fibre. The authors thank the EPSRC Centre for Innovative Manufacturing in Photonics for support.